

# Design and Implementation of a Low Cost Grid-Connected 5 kVA Photovoltaic System with Load Compensation Capability

Reza Seifi Mejdari<sup>†</sup>, Mahdi Salimi<sup>\*</sup>, and Adel Zakipour<sup>\*</sup>

<sup>†,\*</sup>Department of Electrical Engineering, Ardabil Branch, Islamic Azad University, Ardabil, Iran

## Abstract

Design and implementation of a low cost grid-connected 5kVA solar photovoltaic (PV) system is proposed in this paper. Since the inverter is a major component of the PV system, the B4 inverter used in this paper reduces the total cost of the PV system. In order to eliminate the massive transformer, the PV system is connected to the grid through IGBT switches. In addition to injection of active power into the grid, the B4 inverter can compensate reactive power and reduce harmonics of the nonlinear loads. A TMS320F28335 DSP processor is used for effective control of the B4 inverter. Various features of this processor enable the implementation of the necessary control algorithms. As a first step, the PV system is simulated and evaluated in Matlab/Simulink. In the second step, hardware circuits are designed and implemented based on the simulation results. The operation of the PV system has been evaluated under balanced, unbalanced, linear and nonlinear loads which proves its accuracy and efficiency.

**Key words:** B4 inverter, DSP, Grid-connected PV system

## I. INTRODUCTION

Recently due to the rising crisis of traditional energy, the research and application of sustainable energy particularly the PV power generation have been attracted more and more attention [1]. Along with the rising of energy crisis, governments have to pay a lot more attention to sustainable energy resources. The continued growth of electrical energy consumption along with the necessity of a clean environment, demands decentralized renewable energy generation. Increasing energy consumption may overload the distribution grid as well as power stations. In addition, it may have a negative impact on power availability, security and quality. The only solution to solve this problem is integrating renewable energy resources like solar, wind or hydro into the grid.

The grid can be connected to renewable energy systems as per the accessibility of renewable energy resources. Recently more attention has been paid to solar PV systems since solar

energy is widely available, more effective and more environmental friendly when compared to conventional power generation systems such as fossil fuel, coal or nuclear. The main problems with PV systems is that they can only supply a load on sunny days. Therefore, for improving the performance and providing power all day along, it is necessary to hybrid PV systems with other power generation systems or to link them with the utility grid. The integration of PV systems with the grid requires a PWM (pulse width modulation)voltage source converter for interfacing with the grid [2]. Grid-connected solar PV systems employ the direct conversion of sun energy into electricity which is fed directly into the grid without being stored in batteries. This can be a very useful way to improve the existing electricity production capacity, which is mainly from hydro and thermal sources. Solar energy, being a renewable source, also produces energy without pollution or greenhouse gas emissions. This can go a long way to help decrease the harmful effects of global warming as well as contribute to sustainable energy development [3]. The global cumulative scenarios, Moderate and Policy-Driven, according to the EPIA are shown in Fig. 1 [4]. After adding close to 30 GW of PV systems in 2011, the PV market is at a crossroads in its development.

Manuscript received Nov. 28, 2015; accepted Jun. 15, 2016

Recommended for publication by Associate Editor Alian Chen.

<sup>†</sup>Corresponding Author: r.seifi.m@iauardabil.ac.ir

Tel: +98-912-508-4611, Ardabil Branch, Islamic Azad University

<sup>\*</sup>Dept. of Electrical Eng., Ardabil Branch, Islamic Azad University, Iran

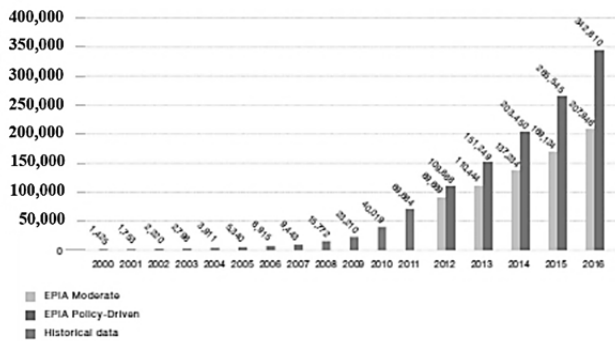


Fig. 1. Global cumulative scenarios until 2016 - Moderate and Policy-Driven (MW). Source: EPIA.

The expected growth of markets outside Europe will not compensate for the slowdown in the European before 2016 in the pessimistic Moderate scenario. This assumes a negative perspective in most markets in the five coming years, especially in Europe. Depending on the conditions of the Moderate scenario, the 100 GW mark could be reached in 2012 or 2013, while according to the Policy-Driven scenario, more than 350 GW of PV systems could be connected to the grid over the next five years. The bulk penetration of PV systems is expected around 2015 when the cost of PV electricity is forecasted to become comparable to the price of conventional energy [5].

The design and implementation of solar PV systems face a lot of complexity, even on a small scale. It must pay a lot of attention to key factors such as optimum active power injection, reactive power, current harmonics and voltage dip compensation, power factor reduction, dynamic response, maximum power point tracking and total cost in order to have an effectively designed PV solar power station. Since beginning of the introduction of solar PV systems, a lot of studies have been done to optimize its different parts including the solar panels, DC-DC converters, DC-AC inverters, control units, etc. A grid-connected PV system is proposed with a high voltage gain [6]. A synchronization technique is used in grid-connected converter control systems to compensate non-ideal supply voltages and to achieve a higher frequency variability [7]. In [8], a simplified reactive power control (SRPC) strategy is proposed for the inverters in single-phase grid-connected PV systems. With this strategy, the current-mode asynchronous sigma-delta modulation (CASDM) is adopted to improve the current control's dynamic response and to reduce both current harmonic distortion and electromagnetic interference. A single-phase, single-stage current source inverter-based system is offered for grid-connected PV systems [9]. A system utilizing transformer-less single-stage conversion is proposed for tracking the maximum power point and for interfacing PV arrays to the grid. In [10], a high-reliability single-phase transformerless grid-connected inverter is presented that uses superjunction MOSFETs to reach a high efficiency for PV

applications. This converter utilizes two separate ac-coupled inductors that operate for positive and negative half grid cycles. This removes the shoot-through issue encountered with traditional voltage source inverters leading to an improved system reliability. Technical and economic efficiencies of different active and reactive power control strategies have been discussed for grid-connected PV systems in Germany [11]. In [12], a new approach for an optimum design of transformerless PV inverters is presented, targeting a cost-effective propagation of grid-connected PV systems. The optimal switching frequency as well as the optimal values and types of PV inverter components is calculated in such a way that the PV inverter levelized cost of electricity (LCOE) is minimized during the PV system lifetime. The LCOE is also calculated concerning the failure rates of the components, which affects the reliability performance and lifetime maintenance cost of the PV inverter. A novel transformerless grid-connected power converter is proposed with a negative grounding for PV generation systems [13]. The negative terminal of a solar cell array in the proposed grid-connected power converter can be directly connected to the ground to neglect the transparent conducting oxide corrosion that take places in some types of thin-film solar cell arrays. The proposed grid-connected power converter includes a DC-DC power converter and a DC-AC inverter. An improved maximum power point tracking (MPPT) with better performance based on voltage-oriented control (VOC) is offered to solve the fast-changing irradiation problem [14]. In VOC, a cascaded control structure is used with an outer DC-link voltage control loop and an inner current control loop. The currents are controlled in the synchronous orthogonal  $d, q$  frame using a decoupled feedback control. Digital control for grid-connected converters has been used to compensate higher frequency variability, non-ideal supply voltage, and ground leakage current [7], [15]. In [16], DSP-based control of grid-connected power converters is proposed to improve operation performance under grid distortions. In addition, there have been a lot of studies to achieve better performance in PV solar power stations.

In this paper design and implementation of a low cost grid-connected 5 kVA PV system is presented. The main contribution of this paper is the design and implementation of a grid-connected PV system with load compensation capability. In fact, it is possible to compensate load harmonic currents and reactive components during active PV power injection into the grid. In addition, the B4 inverter used in this design can considerably reduce the total cost of the PV system. Accordingly, this paper is organized as follows. In section II, the design methodology is proposed, and the required parts and control algorithms are presented. Some simulation results are shown at the end of this section. The hardware implementation is discussed in section III. Operational results under various real conditions can be seen in this section. Finally, some conclusions are described and discussed in section IV.

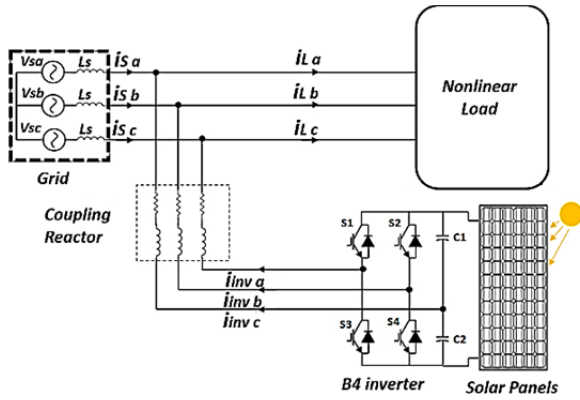


Fig. 2. Grid-connected PV system using B4 inverter.

## II. DESIGNED GRID-CONNECTED PV SYSTEM

### A. Summary of the Grid-Connected PV System

The main structure of a grid-connected PV system is shown in Fig. 2. It has been proved that solar panels can inject maximum power to the grid if they are directly connected, without a DC-DC converter, via a DC-AC inverter. Therefore, the DC-DC converter can be removed and the system efficiency can be increased. The main parts of the PV system are the solar panels; the DC-link; the B4 inverter and the coupling filter for connecting the system to a grid. The capacitors of the DC-link and coupling filter are selected based on the control strategy of the B4 inverter [17]. Basically, a lot of the cost of a grid-connected PV system is related to the DC-AC inverter. Therefore, the B4 inverter used in this paper significantly decreases the total cost of the PV system. There are four IGBT switches in the B4 inverter structure instead of the six IGBT switches in the B6 inverter structure. In addition to a reduction of the IGBT switches, the costs of the startup circuits, snubber circuits, protection circuits and heat sink have been decreased. There are several methods to control the output currents of the B4 inverter. In this paper, the hysteresis current control (HCC) method is used because of its straightforward implementation and fast dynamic response. The operation of a single-phase inverter is shown in Fig. 3(a). In this plot,  $i_{ref}$  is the reference current of the inverter which is supplied through suitable switching in the controller. In addition,  $H$  is the hysteresis band which determines the inverter switching frequency and the current error. In Fig 3(b), when  $S_1$  is turned on, the voltage at the inductor is positive through the upper path. Hence, the inductor current, which is an integral of the current, increases. In the next switching interval, the inductor current decreases due to a negative voltage. According to the status of the power switches in a single-phase inverter, two different modes can be considered: a) If  $S_1$  turns on and  $S_3$  turns off, the inductive load current ( $i_{L,a}$ ) increases. b) If  $S_3$  turns on and  $S_1$  turns off, the inductive load current decreases. It is clear that by applying suitable switching, it becomes possible to control the variations of the output current. As a result, it

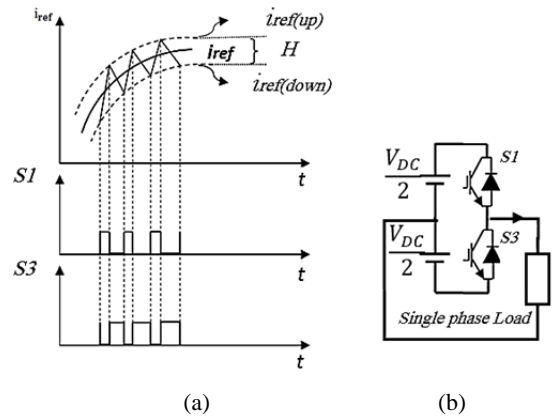


Fig. 3. Single-phase inverter. (a) Principles of the HCC method (b) Single-phase half bridge inverter.

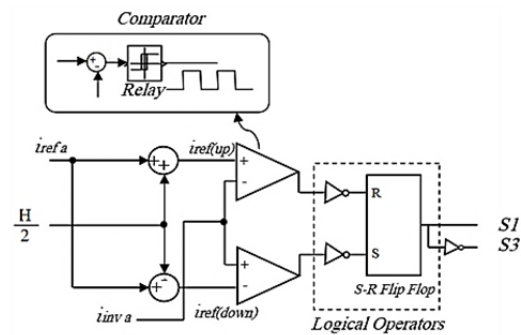


Fig. 4. Implementation of the HCC method (single phase, a).

always lies in a specific range.

This can be achieved by defining  $H$  around the  $i_{ref}$ :

$$\begin{cases} i_{ref(up)} = i_{ref} + \frac{H}{2} \\ i_{ref(down)} = i_{ref} - \frac{H}{2} \end{cases} \quad (1)$$

In the HCC method, the output current of the inverter is compared with  $i_{ref(up)}$  and  $i_{ref(down)}$  (Fig. 4). It is clear that a reduction of the hysteresis band decreases the output error. On the other hand, the switching frequency and power losses will be increased. In this paper, a fixed hysteresis band is used to control the comparators.

Startup circuits are used for primary switching of the IGBT switches. The inverter is protected against the following faults: a) An increase in the peak output current. b) An increase in the average output current. c) An increase and decrease in the capacitor voltage of the DC-link. d) An increase in the heat sink temperature.

In the HCC method, the reference current is bounded to a specific range. Therefore, the output current does not exceed the upper or lower range.

In addition, a LM35 temperature sensor is considered for the heat sink to measure the temperature. The upper range temperature for the heat sink is adjusted to 80°C. Protection against high and low voltages of the capacitors in the DC-link

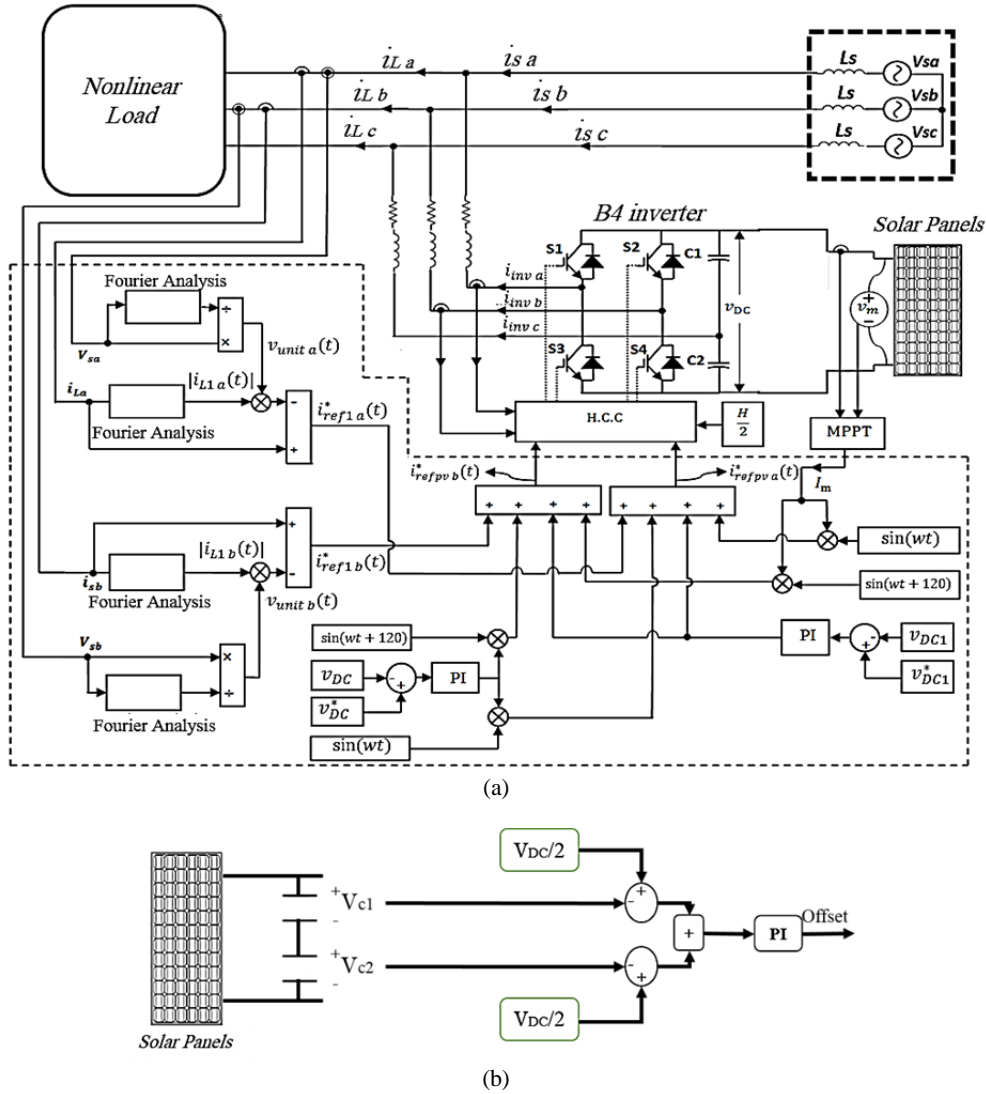


Fig. 5. Grid-connected PV system. (a) The control strategy of the grid-connected PV system. (b) subcontroller of DC-link.

is considered. Therefore, the inverter turns off if the capacitor voltage falls and the output current exceeds a specific threshold. Since the upper range of the capacitor voltage is high, about 800V, an isolated sampling circuit is used in this system.

### B. Control Strategy of the Inverter

In addition, to inject active power from the solar panels to the grid, and to provide reactive power for the local loads, the PV system can compensate the harmonics of the load current. The operation of the grid-connected PV system is fully depends on the control strategy of the voltage source inverter (VSI). This control strategy produces a reference current and stabilizes the capacitor voltage of the DC-link.

The main structure of the control strategy is shown in Fig. 5. The reactive instantaneous power theory, proposed by Akagi, is used to calculate the reference current [18]. The active power is injected into the grid by the solar panels. Furthermore, the reactive power and harmonics of the load currents are compensated with the B4 inverter. The reference currents in the

$\alpha\beta$  coordinates are as follows:

$$\begin{bmatrix} i_{\alpha}^* \\ i_{\beta}^* \end{bmatrix} = \frac{1}{v_{\alpha}^2 + v_{\beta}^2} \begin{bmatrix} V_{\alpha} & V_{\beta} \\ V_{\beta} & -V_{\alpha} \end{bmatrix} \begin{bmatrix} \tilde{p}_L & p_{active} \\ \tilde{q}_L & \tilde{q}_L \end{bmatrix} \quad (2)$$

where  $V_{\alpha}, V_{\beta}$  are the load voltages,  $i_{\alpha}^*, i_{\beta}^*$  are the reference currents and  $\tilde{p}_L, \tilde{q}_L$  are the instantaneous power of the load in the  $\alpha\beta$  coordinates.  $p_{active}$  is the output of the DC-link controller. On the other hand, the reference currents in the  $abc$  coordinates are as follows:

$$\begin{bmatrix} i_a^* \\ i_b^* \\ i_c^* \end{bmatrix} = \sqrt{\frac{3}{2}} \begin{bmatrix} 1 & 0 \\ -1/2 & \sqrt{3}/2 \\ -1/2 & -\sqrt{3}/2 \end{bmatrix} \begin{bmatrix} i_{\alpha}^* \\ i_{\beta}^* \end{bmatrix} \quad (3)$$

If the output currents of the inverter are equal to  $i_a^*$  and  $i_b^*$ , concerning the formation of  $i_c^*$  in a neutral wire without switching, the power produced by the solar panels is injected into the grid. This process makes the input capacitor voltage fixed. The inverter provides harmonic currents and reactive power. Therefore, the power factor remains near unity. Consequently, the harmonic currents cannot enter the grid. If the power generated by the solar panels is low, the controller of

TABLE I  
MAIN PARAMETERS IN SIMULATED MODEL

Components & Parameters	Rating Value
Phase to neutral voltage of the grid	220 volt
Ref. voltage of the DC-link capacitor	800 volt
DC-link capacitors	1000 $\mu$ F
Grid-connected inductance	2.2 mH
Switching frequency	16 kHz

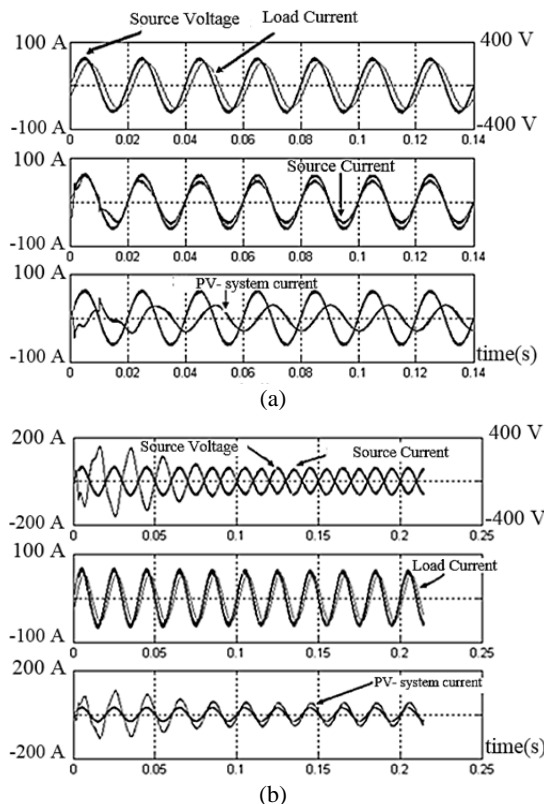


Fig. 6. Grid-connected PV system with RL load. (a) Reactive power compensation, (b) Active power injection.

the capacitor can receive some active power from the grid until the capacitor voltage stops dropping. In this case, the PV system is able to provide reactive power and harmonic currents.

### C. Simulation Results

In this section, simulation results of the discussed control strategy for grid-connected PV systems is presented. MatlabR15/Simulink software is used for the simulations. The main parameters of the simulated model are shown in Table I.

In the first experiment, the RL load was tested. The simulation results are shown in Fig. 6. In Fig. 6(a), it is assumed that the power generated by the solar panels is low and that the grid-connected PV system only produces reactive power for the load. The active power consumption of the load is supplied from the grid. In Fig. 6(b) it is supposed that the power generated by the solar panels is higher than the power

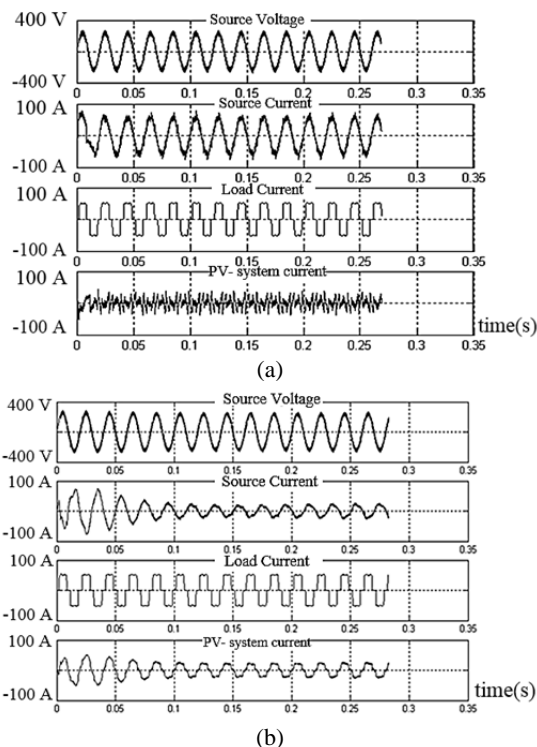


Fig. 7. Grid-connected PV system with nonlinear load. (a) Reactive power compensation, (b) Active power injection.

required for the load. Therefore, in addition to active and reactive power for the load, the PV system injects extra active power into the grid.

In the second experiment, to investigate the harmonics compensation by the PV system, a three-phase full-bridge diode is used as a nonlinear load. The simulation results show that in spite of the harmonic currents and reactive power consumed by the load, the current drawn from the grid (Fig. 7(a)) and the current injected into the grid (Fig. 7(b)) are nearly sinusoidal and in phase with the line voltage.

## III. IMPLEMENTED PROTOTYPE AND EXPERIMENTAL RESULTS

A 5 kVA prototype of the proposed grid-connected PV system has been implemented. The control unit for this system has been programmed in the DSP based control unit discussed below.

### A. DSP based Control Unit

A Texas Instruments (TI) DSP processor, TMS320F28335, is used in the control circuit [19]. This is a 32-bit floating-point processor with a 12-bit ADC. The sampling frequency of the analog parameters, currents and voltages, is 50 kHz. The main loop of the DSP program is also performed at 50 kHz. A flowchart of the DSP control algorithm is shown in Fig. 8.

The first step in the TMS320F28335 operation is initializing. In this step, the registers of the DSP, the PLL, and the DSP clock are initialized. In addition, the A/D converter and the

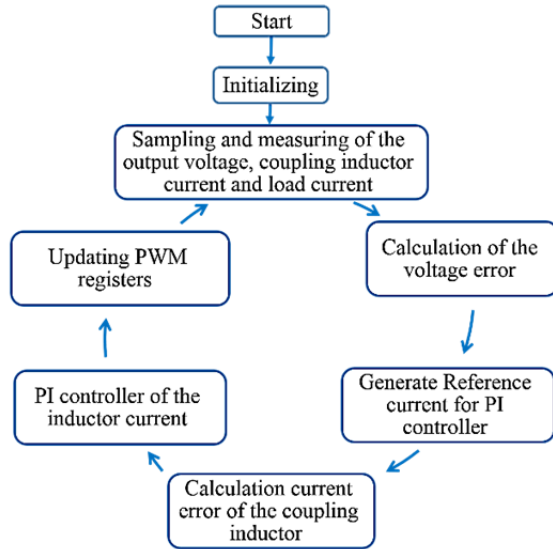


Fig. 8. Flowchart of the DSP control algorithm.

PWM are set-up and the interrupts are adjusted. After initializing, samples are taken from the DC-link and grid voltages. In step 3, the DC-link voltage is compared with a reference voltage and the voltage error is calculated. Accordingly, a reference voltage is prepared for the PI controller. Then, the coupling inductor current is compared with the reference current and an error current is produced. In step 6, accurate commands are provided for the PI controller. In the last step, the PWMs are updated. Finally, the control loop goes back to step 3, and step 3 to step 8 operate in a repetitive loop.

**B. Components and Hardware of the PV System Unit**

The main tested hardware is shown in Fig. 9. The operation of each piece of equipment is shown in the photograph. The components and parameter details are listed in Table II.

TABLE II  
EXPERIMENTAL TEST BENCH SPECIFICATIONS

Description	Specifications
solar Panel	40 panel (in series); 100W; 5A; 22.5V
DC-link capacitors	1000 $\mu$ F
IGBTs	BUP314 (1200V, 42A)
Switching frequency	16 kHz with 2 $\mu$ s dead time
Coupling Inductors	2.2 mH (iron core with 0.68 $\Omega$ parasitic resistance)
Linear test Load	Series RL with L=46 mH and R=30 $\Omega$
Nonlinear test load	Bridge-Rectifiers (KBU8M) series with C=500 $\mu$ F and R=26 $\Omega$ , 40 $\Omega$ .
Current sensors	LA100 from LEM Co.

**C. Experimental Results**

To evaluate the performance of the PV system, numerous experiments have been carried out. Here, the results of 5 experiments are represented. The first set of experimental results is shown in Fig. 10. This experiment shows the inverter response to variations of the DC-link capacitor voltage (voltage loop test). In this experiment, the inverter input voltage changes between 350 V and 500 V per 0.5 second intervals. The frequency of the inverter is 16 KHz. It can be properly concluded that the inverter follows these changes based on the inverter current waveform.

In the second experiment, a nonlinear load is evaluated (Fig. 11). Therefore, the inverter input voltage is considered to be 420V and a combination of capacitors, resistors and the bridge rectifier is used as a nonlinear load. The experiment results are shown in Fig. 11. In this figure, both the reference and inverter current can be seen. The inverter follows the reference current properly.

The reactive power provided by the PV system is evaluated in the third experiment. In this experiment, it is assumed that the solar panels cannot produce active power (night mode) and

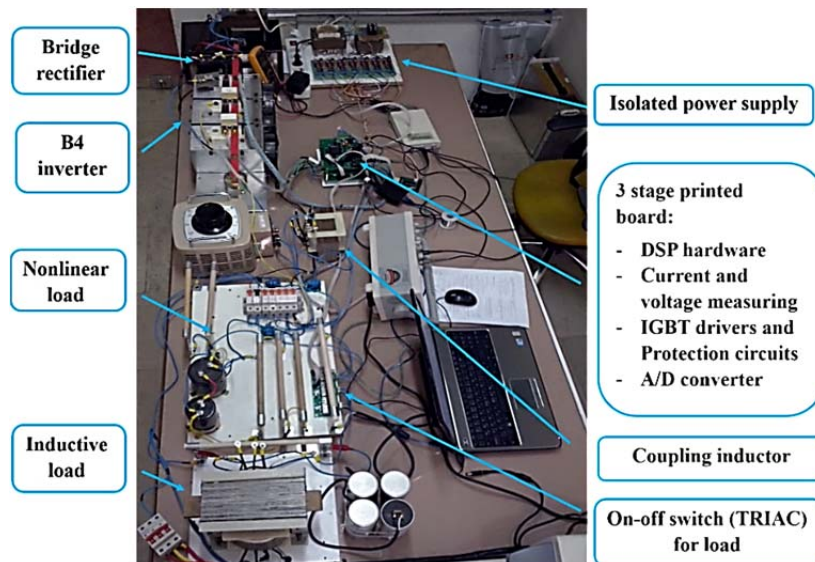


Fig. 9. Experimental setup photo.

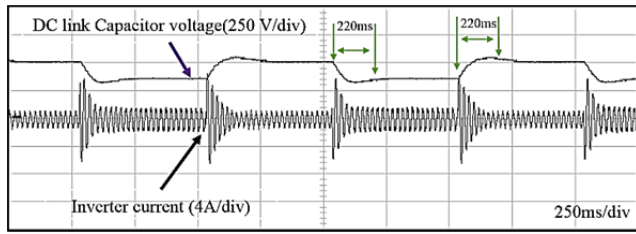


Fig. 10. Input voltage variation of the B4 inverter (voltage loop test).

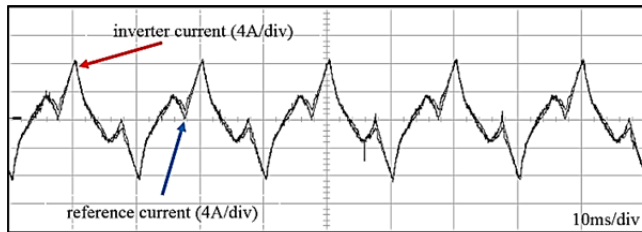


Fig. 11. PV system under nonlinear load(current loop test).

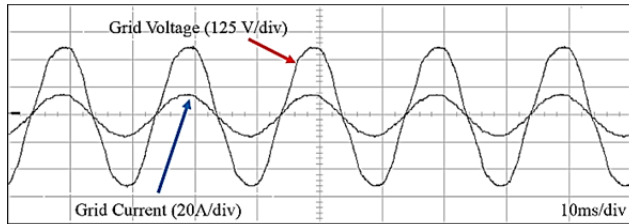


Fig. 12. PV system in night mode supplies reactive power.

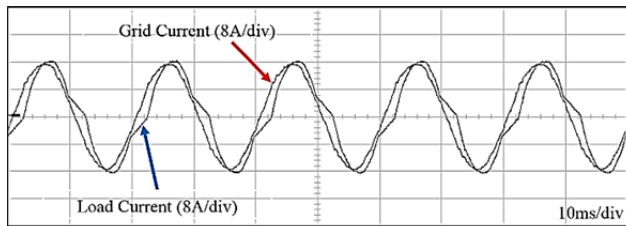


Fig. 13. Grid and load current in night mode.

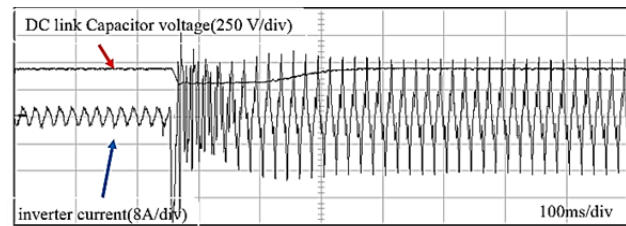


Fig. 14. Connecting load to the PV system.

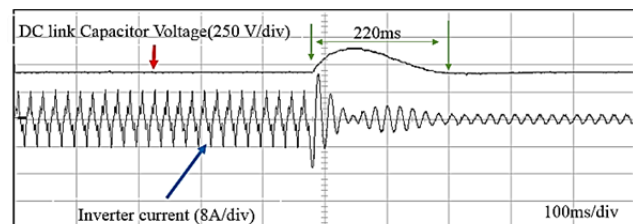
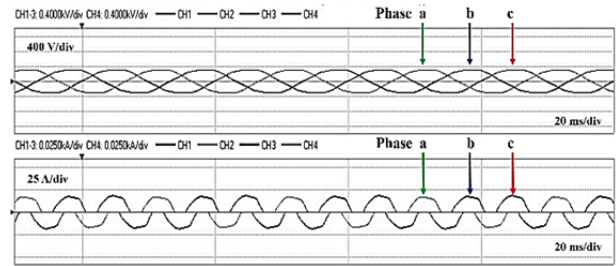
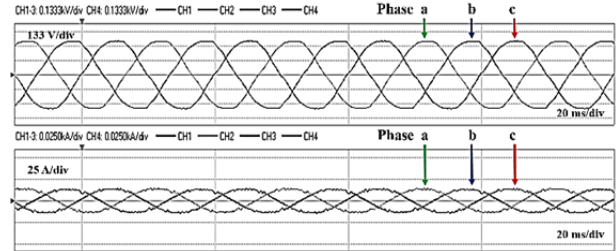


Fig. 15. Load disconnected of PV system.



(a)



(b)

Fig. 16. Reactive power compensation by PV system. (a) before compensation (b) after compensation.

that the required active power is supplied by the grid. In this case, the PV system provides the reactive power of the load.

In Fig. 12, both the semi-sinusoidal voltage and current of the grid are shown. The grid sinusoidal current and the load non-sinusoidal current are shown in Fig. 13. The difference between these two currents is supplied by the inverter.

In the fourth experiment, the load is applied to the PV system and then disconnected. As shown in Figure. 14, until the load remains disconnected, the inverter is disabled. After applying the load, the inverter starts working and provides power for the load. Then, the inverter is disabled when the load is disconnected (Fig. 15). In this experiment, the inverter input voltage is considered to be 420V. This voltage has a swing in the time of applying and disconnecting the load and then returns to the steady state.

In the last experiment, the reactive power compensation by the PV system is investigated. Therefore, a nonlinear load is connected to the PV system. The three-phase voltages and currents of the grid (50 Hz) are shown before and after the compensation (Fig.16).

#### IV. CONCLUSIONS

In this paper, the design and implementation of a 5 kVA grid-connected PV system is proposed. The B4 inverter used in this system considerably reduces the total cost of the system. In addition to injecting active power (day mode), the inverter can compensate the reactive power of the load (night mode). A TMS320F28335 DSP processor is used to control the operation of the system. Due to the numerous capabilities of this processor, it is possible to implement different control algorithms. The system is initially tested in Matlab/Simulink software. After obtaining the desired results, a hardware model

has been constructed. Experimental results show satisfactory behavior under various working conditions.

#### ACKNOWLEDGMENT

This research was supported by the Islamic Azad University, Ardabil Branch under a Research Grant.

#### REFERENCES

- [1] R. A. Messenger and J. Ventre, *Photovoltaic Systems Engineering*, Third Edition, CRC Press, Taylor & Francis Group, Chapter 1, 2010.
- [2] G. Stapleton and S. Neill, *Grid-connected Solar Electric Systems: The Earthscan Expert Handbook for Planning, Design and Installation*, Earthscan, Chapter 1, 2012.
- [3] E. N. Kumi and A. B. Hammond, *Design and Analysis of a 1MW Grid-Connected Solar PV System in Ghana*, African Technology Policy Studies Network, Working Paper series, Chapter 2, 2013.
- [4] EPIA, "Global market outlook for photovoltaics until 2016," [http://www.pv-magazine.com/fileadm/uploads/PDFs/Global\\_Market\\_Outlook\\_2016.pdf](http://www.pv-magazine.com/fileadm/uploads/PDFs/Global_Market_Outlook_2016.pdf), May 2012.
- [5] R. Teodorescu, M. Liserre, and P. Rodríguez, *Grid Converters for Photovoltaic and Wind Power Systems*, Wiley, John Wiley&Sons, Chapter 1, 2011.
- [6] B. Yang, W. Li, Y. Zhao, and X. He, "Design and analysis of a grid-connected photovoltaic power system," *IEEE Trans. Power Electron.*, Vol. 25, No. 4, pp. 992-1000, Apr. 2010.
- [7] H. L. Ginn and G. Chen, "Digital control method for grid-connected converters supplied with nonideal voltage," *IEEE Trans. Ind. Informat.*, Vol. 10, No. 1, pp. 127-136, Feb. 2014.
- [8] C. H. Chang, Y. H. Lin, Y. M. Chen, and Y. R. Chang, "Simplified reactive power control for single-phase grid-connected photovoltaic inverters," *IEEE Trans. Ind. Electron.*, Vol. 61, No. 5, pp. 2286-2296, May 2014.
- [9] B. N. Alajmi, K. H. Ahmed, G. P. Adam, and B. W. Williams, "Single-phase single-stage transformer less grid-connected PV system," *IEEE Trans. Power Electron.*, Vol. 28, No. 6, pp. 2664-2676, Jun. 2013.
- [10] B. Gu, J. Dominic, J. S. Lai, C. L. Chen, T. LaBella, and B. Chen, "High reliability and efficiency single-phase transformerless inverter for grid-connected photovoltaic systems," *IEEE Trans. Power Electron.*, Vol. 28, No. 5, pp. 2235-2245, May 2013.
- [11] T. Stetz, F. Marten, and M. Braun, "Improved low voltage grid-integration of photovoltaic systems in Germany," *IEEE Trans. Sustain. Energy*, Vol. 4, No. 2, pp. 534-542, Apr. 2013.
- [12] E. Koutroulis and F. Blaabjerg, "Design optimization of transformerless grid-connected PV inverters including reliability," *IEEE Trans. Power Electron.*, Vol. 28, No. 1, pp. 325-335, Jan. 2013.
- [13] J. M. Shen, H. L. Jou, and J. C. Wu, "Novel transformerless grid-connected power converter with negative grounding for photovoltaic generation system," *IEEE Trans. Power Electron.*, Vol. 27, No. 4, pp. 1818-1829, Apr. 2012.
- [14] R. Kadri, J. P. Gaubert, and G. Champenois, "An improved maximum power point tracking for photovoltaic grid-connected inverter based on voltage-oriented control," *IEEE Trans. Ind. Electron.*, Vol. 58, No. 1, pp. 66-75, Jan. 2011.
- [15] G. Buticchi, D. Barater, E. Lorenzani, and G. Franceschini, "Digital control of actual grid-connected converters for ground leakage current reduction in PV transformerless systems," *IEEE Trans. Ind. Informat.*, Vol. 8, No. 3, pp. 563-572, Aug. 2012.
- [16] M. P. Kazmierkowski, M. Jasinski, and G. Wrona, "DSP-based control of grid-connected power converters operating under grid distortions," *IEEE Trans. Ind. Informat.*, Vol. 7, No. 2, pp. 204-211, May 2011.
- [17] F. M. Ishengoma and L. N. Norum, "Design and implementation of digitally controlled stand-alone photovoltaic power supply," in *Nordic Workshop on Power and Industrial Electronics (NORPIE)*, pp. 741-744, Aug. 2002.
- [18] H. Akagi, Y. Kanazawa, and A. Nabae, "Instantaneous reactive power compensators comprising switching devices without energy storage components," *IEEE Trans. Ind. Appl.*, Vol. IA-20, No. 3, pp. 625-630, May 1984.
- [19] TMS320F28335, <http://www.ti.com/lit/ds/symlink/tms320f28335.pdf>, Aug. 2012.
- [20] H. H. Moghaddam and M. salami, "Applicability improvement and hysteresis current control method simplification in shunt active filters," in *IJEEE*, Vol. 11, No. 3, pp.276-283, 2015.



**Reza Seifi Mejdari** was born in Hashtpar, Iran, in 1978. He received his B.S. degree in Electrical Engineering from the Amirkabir University of Technology, Tehran, Iran, in 2001; and his M.S. degree in Electrical Engineering from Shahid Beheshti University, Tehran, Iran, in 2004. He is presently working towards his Ph.D. degree

in the Science and Research Branch of the Islamic Azad University, Tehran, Iran. Since 2006, he has been with the Islamic Azad University. His current research interests include renewable energy and the design and fabrication of digital circuits and systems.



**Mahdi Salimi** was born in Ardabil, Iran, in 1979. He received his B.S. and M.S. degrees in Electrical Engineering from the K.N.T. University of Technology, Tehran, Iran, in 2000 and 2002, respectively; and his Ph.D. degree in Power Electronics from Science and Research Branch, Islamic Azad University, Tehran, Iran, in 2012. Since 2003,

he has been with the Islamic Azad University, where he is presently working as an Assistant Professor in the Department of Electrical Engineering. His current research interests include the closed-loop control of power electronics converters, high gain DC-DC converters, grid-connected inverters, and renewable energy.





**Adel Zakipour** was born in Ardabil, Iran, in 1981. He received his B.S. degree in Electrical Engineering from the Islamic Azad University, Ardabil, Iran, in 2002; and his M.S. degree in Electrical Engineering from the Iran University of Science and Technology, Tehran, Iran, in 2004. He is presently working toward his Ph.D. degree at the K.N.T. University of Technology, Tehran, Iran. Since 2005, he has been with the Islamic Azad University. His current research interests include power electronics, electrical machine drives, grid-connected inverters and their application in renewable energy systems.